Maternal Obesity Induces Epigenetic Modifications to Facilitate Zfp423 Expression and Enhance Adipogenic Differentiation in Fetal Mice

Qi-Yuan Yang,[1,2] Jun-Fang Liang,[1] Carl J. Rogers,[1] Jun-Xing Zhao,[2] Mei-Jun Zhu,[2,3] and Min Du[1,2]

Maternal obesity (MO) predisposes offspring to obesity and type 2 diabetes despite poorly defined mechanisms. Zfp423 is the key transcription factor committing cells to the adipogenic lineage, with exceptionally dense CpG sites in its promoter. We hypothesized that MO enhances adipogenic differentiation during fetal development through inducing epigenetic changes in the Zfp423 promoter and elevating its expression. Female mice were subjected to a control (Con) or obesogenic (OB) diet for 2 months, mated, and maintained on their diets during pregnancy. Fetal tissue was harvested at embryonic day 14.5 (E14.5), when the early adipogenic commitment is initiated. The Zfp423 expression was 3.6-fold higher and DNA methylation in the Zfp423 promoter was lower in OB compared with Con. Correspondingly, repressive histone methylation (H3K27me3) was lower in the Zfp423 promoter of OB fetal tissue, accompanied by reduced binding of enhancer of zeste 2 (EZH2). Gain- and loss-of-function analysis showed that Zfp423 regulates early adipogenic differentiation in fetal progenitor cells. In summary, MO enhanced Zfp423 expression and adipogenic differentiation during fetal development, at least partially through reducing DNA methylation in the Zfp423 promoter, which is expected to durably elevate adipogenic differentiation of progenitor cells in adult tissue, programming adiposity and metabolic dysfunction later in life. ***Diabetes*** **62:3727–3735, 2013**

According to the latest National Health and Nutrition Examination Survey (NHANES; 2009–2010), 31.9% of nonpregnant women 20–39 years of age in the U.S. are obese, and another one-third are overweight (1). Maternal obesity (MO) represents a special problem that can result in poor fetal development, leading to harmful, persistent effects in offspring, including predisposition to obesity and type 2 diabetes (T2D) (2–5). Indeed, T2D and obesity are increasing at alarming rates in teenagers and even children (6). Mechanisms linking MO to the increased incidence of obesity and T2D in their descendants remain poorly defined.

Obesity, especially central obesity, is well correlated with diabetes, hyperlipidemia, and cardiovascular diseases (7). Visceral fat, especially epididymal fat, is the first fat depot to develop, mainly between birth and 4 weeks of age in rodents (8). Adipocyte number in epididymal fat increases little after weaning (9), and further development is primarily due to adipocyte hypertrophy (8). Similarly, in humans, morbid adiposity only slightly elevates visceral adipocyte number (10). Therefore, visceral fat is developed mainly during the late fetal and nursing stages, when the mother provides all nutrients. As a result, MO is expected to enhance adipogenesis and visceral fat development. Indeed, a recent study using magnetic resonance imaging found that MO correlates with abdominal adiposity in human neonates (11), consistent with enhanced central adiposity in the offspring of obese mice (12,13).

Skeletal muscle composes ~40–50% of the body mass of adults, and insulin resistance in skeletal muscle is indispensable for the incidence of T2D (14). Intramuscular fatty accumulation leads to muscle insulin resistance (15,16). In addition, it also impairs muscle contractile function, resulting in muscle weakness and even immobility (17). MO enhanced intramuscular adipogenesis in fetal muscle, which is associated with higher intramuscular fat content and visceral adiposity in offspring, providing another relationship between MO and the increased incidence of obesity and T2D in offspring (5,13,18). Up until now, mechanisms leading to enhanced adipogenesis in progeny due to MO remain poorly defined.

Adipogenic differentiation has been studied for decades, and 3T3-L1 cells are the major model for studying adipogenesis. Peroxisome proliferator–activated receptor γ (PPARγ) and CCAAT enhancer–binding proteins (C/EBPs) act as critical regulators of adipogenic differentiation (19). Quite recently, zinc-finger protein Zfp423 was discovered to initiate the early preadipocyte commitment in mature adipose tissue, which induces PPARγ expression and adipogenic differentiation (20). It remains unclear whether Zfp423 regulates adipogenesis during fetal development and how Zfp423 expression is regulated. We speculated that during adipose tissue development, Zfp423 expression is regulated primarily through epigenetic modifications.

Cell differentiation, including adipogenesis, involves epigenetic modifications. The Polycomb repressive complex 2 (PRC2) has histone methyltransferase activity due to the presence of enhancer of zeste 1 and 2 (EZH1/2), which catalyzes histone 3 lysine 27 trimethylation (H3K27me3), a marker for gene silencing (21). Although no specific DNA binding element for PRC2 has been identified, PRC2 tends to bind promoters with rich GC sites, which attracts PRC1 binding (22). The trithorax group (trxG) catalyzes H3K4 trimethylation (H3K4me3), which activates gene transcription (23). Interestingly, H3K4me3 and H3K27me3 coexist, forming a "bivalent state" (24), which poises genes for activation or inhibition. During cell differentiation, non-induced bivalent genes lose active H3K4me3 but keep repressive H3K27me3 mark, leading to a largely permanent inhibition of gene expression by inducing DNA methylation (25). De novo DNA methylation serves to convert plastic

From the [1]Department of Animal Sciences, Washington State University, Pullman, Washington; the [2]Developmental Biology Group, Department of Animal Science, University of Wyoming, Laramie, Wyoming; and the [3]School of Food Science, Washington State University, Pullman, Washington.
Corresponding author: Min Du, min.du@wsu.edu.
Received 18 March 2013 and accepted 16 July 2013.
DOI: 10.2337/db13-0433

gene inhibition by PRCs to permanent silencing (25). Our bioinformatic analyses showed that the Zfp423 promoter presents exceptionally rich CpG sites and islands, meeting the characteristics of a "key developmental gene" with high CpG density promoters (24). Because Zfp423 is a critical transcription factor initiating adipogenic commitment, we hypothesized that MO enhances Zfp423 expression and adipogenic differentiation during fetal development via attenuating DNA methylation and inhibitory histone modifications in the Zfp423 promoter.

RESEARCH DESIGN AND METHODS

Animals. Animal studies were conducted according to the protocol approved by the Animal Use and Care Committees of both the University of Wyoming and Washington State University. The diet-induced obesity model was used. Female C57BL/6J mice (4 weeks of age) were fed ad libitum either a control diet (D12450B; Research Diets, New Brunswick, NJ) with 10% energy from fat (Con) or a high-energy diet (D12451) with 45% energy (OB) from fat for 8 weeks at 12-h light/12-h dark cycles. Then, both Con and OB female mice were mated with C57BL/6J male mice (on the normal rodent diet), and mating was confirmed by the presence of a vaginal plug. During pregnancy, each female was individually housed. At E14.5, mice were killed and fetuses were collected and weighed. Then, under a dissecting microscope, fetal tissue was harvested after removing the head, heart, lung, and liver; surface gelatinous tissue; and spinal cord and primordial bones. Due to the small size, fetal tissue from the same litter was pooled, and the litter was considered as an experimental unit.

Real-time quantitative PCR. Real-time quantitative PCR was conducted as previously described. Primer sequences and the amplicon sizes are listed in Table 1. Relative expression of mRNA was determined after normalization to the 18S reference using the ΔΔ-Ct method (26).

Western blot analysis. Western blotting was conducted as previously described (26). Polyclonal antibody against Zfp423 was purchased from Santa Cruz, against EZH2 from Cell Signaling Technology (Boston, MA), and against β-actin from Earthox (San Francisco, CA).

Genomic DNA isolation and sodium bisulfite sequencing. Genomic DNA was extracted using the phenol-chloroform method. Genomic DNA was modified with sodium bisulfite using the EZ DNA Methylation Kit (Zymo Research, Irvine, CA). The MethPrimer software was used to search CpG islands and design primers (27). Primers specific to the bisulfite-modified sequences of the Zfp423 promoter region are listed in Table 1.

The Silica Bead DNA Gel Extraction Kit was purchased from Fermentas (Thermo Fisher Scientific, Waltham, MA). The pGEM-T Easy Vector System (Promega, Madison, WI) was used to clone bisulfite-modified sequences via TA cloning. Plasmids were extracted using a GeneJET Plasmid Miniprep Kit (Thermo Fisher Scientific). DNA methylation status was evaluated by comparing the cloned sequence against the genomic sequence, and the methylation map was generated using Quantification Tool for Methylation Analysis (QUMA, Kyoto, Japan) (28).

Embryonic fibroblast preparation and adipogenic induction. Mouse embryonic fibroblasts (MEFs) were separated from E14.5 fetal mice according to a common procedure, as previously described with slight modifications (29–32). In brief, fresh tissue separated under a stereomicroscope was minced and digested in medium containing 0.75 units/mL collagenase D (Roche, Pleasanton, CA) and 1.0 unit/mL Dipase type II (Roche) for 20 min at 37°C. The lysate was filtered sequentially through 70- and 40-μm cell strainers. The adipogenic differentiation was induced using a medium containing 0.5 mmol/L isobutyl-1-methylxanthine, 1 μmol/L dexamethasone, and 5 μg/mL insulin in Dulbecco's modified Eagle's medium with 15% FBS for 8 days and changed to insulin-only (5 μg/mL) Dulbecco's modified Eagle's medium with 10% FBS for 4 more days (26).

Progenitor cells were further sorted using surface markers, Sca-1$^+$/CD45$^-$, by Magnetic Cell Sorting System (MACS). The antibody MicroBeads kit and MACS separation column were bought from Miltenyi Biotec (Auburn, California). Sca-1$^+$ marks a group of progenitor cells with high adipogenic potential (33,34), whereas CD45$^+$ cells are of blood origin (33). Adipogenic differentiation was induced in sorted cells as described above.

Oil Red O staining of differentiated adipocytes. Cells were fixed and stained with Oil Red O (Sigma-Aldrich, St. Louis, MO) as described previously (26). After microscopic observation, Oil Red O dye was solubilized with isopropanol, and the light absorbance was measured at 510 nm.

Chromatin immunoprecipitation assay. Fetal tissue was homogenized in 1% formaldehyde solution and incubated for 10 min and centrifuged. The pellet was resuspended in PBS containing 125 mmol/L glycine. After centrifuge, the pellet was lysed in a cold lysis buffer (1% SDS, 10 mmol/L Tris-HCl, pH 8.0, 10 mmol/L NaCl, 3 mmol/L $MgCl_2$, and 0.5% NP-40) containing 10 μL protease inhibitor cocktail (Thermo Fisher Scientific), sonicated, and centrifuged. The supernatant was precleaned with chromatin immunoprecipitation (ChIP)–grade protein G (Cell Signaling Technology) and then incubated with an antibody against H3K27me3, H3K4me3, EZH2, H3K9ac, or H3K27ac (Cell Signaling), or normal rabbit IgG overnight at 4°C. Then, the antibody-chromatin complex was precipitated with protein G and further treated with RNaseA (fermentas) and then proteinase K for 2 h. DNA was purified with ChIP DNA Clean & Concentrator (Zymo Research) and used as templates for PCR using the primers listed in Table 1. Relative enrichment folds of detected proteins were determined after normalization to input DNA using the ΔΔ-Ct method.

Plasmid and transfection in vitro. Plasmid pMSCVFLAG-ZFP423 (catalog no. 24764) and pMKO.1-Zfp423 (catalog no. 35972) were obtained from Addgene (Cambridge, MA). Plasmid transfection was performed using PolyJet in vitro DNA transfection reagent (SignaGen Laboratory, Ijamsville, MD) according to the manufacturer's instructions.

Statistical analyses. Each pregnancy was considered as an experimental unit. Data were analyzed as a complete randomized design using GLM (General Linear Model of Statistical Analysis System; SAS, 2000). The differences in the mean values were compared by Student t test, and mean ± SEs were reported. Statistical significance was considered as $P < 0.05$.

RESULTS

Maternal and fetal body weights. After 2 months feeding on a high-energy diet, OB mice were heavier than Con mice (Con vs. OB, 17.44 ± 0.21 vs. 23.18 ± 0.24 g, $P < 0.01$), which maintained until E14.5, when maternal mice were killed (Con vs. OB, 30.32 ± 1.08 vs. 35.40 ± 1.01 g, $P < 0.05$), consistent with our previous report (13). There was no difference in fetal weight between treatments (Con vs. OB, 0.50 ± 0.03 vs. 0.52 ± 0.03 g).

MO enhanced Zfp423 expression and adipogenic differentiation in OB fetal tissue. In this study, we chose E14.5 fetal tissue for analyzing adipogenesis and Zfp423 epigenetic modifications. Although white adipocytes are not detectable in fetal mice at this stage, molecular changes associated with the early stage of commitment

TABLE 1
Primers used for real-time quantitative PCR and bisulfate sequencing

Name	Forward	Reverse	Amplicon sizes (bp)
Zfp423	GTCACCAGTGCCCAGGAAGAAGAC	AACATCTGGTTGCACAGTTTACACTCAT	144
Zfp423-ChIP1	CCATCATAATTTCCAAACCAGGCAT	GTCCGGAGCGCAGGAGCTTAGTA	146
Zfp423-ChIP2	TGTATTTCCAGCGCTGTCCATCG	CAGGAGGATGTGAGGAGCGGAGT	131
MethPrimer Sec1	GGTTTTATTATGTGTTTTTGTAGTGTA	CTAACTACCTCCATAAACCAAAAACT	265
MethPrimer Sec2	GTTTTTGGTTTATGGAGGTAGTTAG	ATATCCCTCAACTCAACCTACTTAA	322
MethPrimer Sec3	TTGTATAAAAATTCGGTAAGGGG	CCTCCCTATAAAAAACAACCCT	292
MethPrimer Sec4	GGATGTTTTAGAGGTTGGTAGTTT	ACAAACAATAAACTCCTAACGAAAC	225
18S	GTAACCCGTTGAACCCCATT	CCATCCAATCGGTAGTAGCG	151
EZH2	AGTATGACTGCTTCCTACATCCCTTCCAT	AGATGCTGGTAACACTGTGGTCCACA	112

to adipogenesis have initiated, and thus fetal tissue at this stage is ideal for testing preadipocyte commitment and the early events of adipogenic differentiation. Indeed, the expression of Zfp423, the initiator of adipogenic commitment, was very high in E14.5 fetal tissue but was absent when assayed on E9.5 and had only weak expression on postnatal day 0 (P0) (Fig. 1*A*). On the other hand, the expression of PPARγ2, a marker of differentiated adipocytes, was undetectable in fetal tissue at E14.5, showing that there were no differentiated adipocytes (Fig. 1*A*).

Compared with Con pregnancy, the Zfp423 mRNA expression was >3.6-fold greater in OB fetal tissue (Fig. 1*B*). Similarly, Zfp423 protein content was also higher (Fig. 1*C* and *D*), showing that the Zfp423 expression was enhanced in OB fetal tissue.

MO enhanced the Zfp423 expression and adipogenic differentiation in OB progenitor cells. To analyze whether there was an overall difference in adipogenic commitment and adipogenesis, we prepared MEFs from fetal tissue; as demonstrated in previous studies, MEFs contain a large number of progenitor cells and have high adipogenic capacity (29–31), and primary MEFs do not express PPARγ (20). These cells were passaged once, and adipogenesis was induced with an adipogenic cocktail. The Zfp423 expression was higher in OB compared with Con MEFs during the whole 12 days of adipogenic differentiation. Correspondingly, the expression of PPARγ2 was clearly detectable after 6 days of differentiation, with OB higher than Con MEFs (Fig. 2*A*). After 12 days of adipogenic differentiation, many more adipocytes were detected in OB compared with Con MEFs (Fig. 2*B* and *C*). Because these cells have been cultured in vitro for numerous cell generations, the difference in their adipogenic differentiation strongly indicates that MO had long-term promoting effects on the adipogenic differentiation of MEFs in OB fetal tissue.

Because MEFs contain cells at various stages of early commitment and differentiation, we further sorted MEFs using Sca-1$^+$/CD45$^-$ as surface markers. Sca-1$^+$ marks a group of progenitor cells with high adipogenic potential (33) whereas CD45$^+$ cells are of blood origin (34). After 12 days of adipogenic differentiation, more adipocytes were

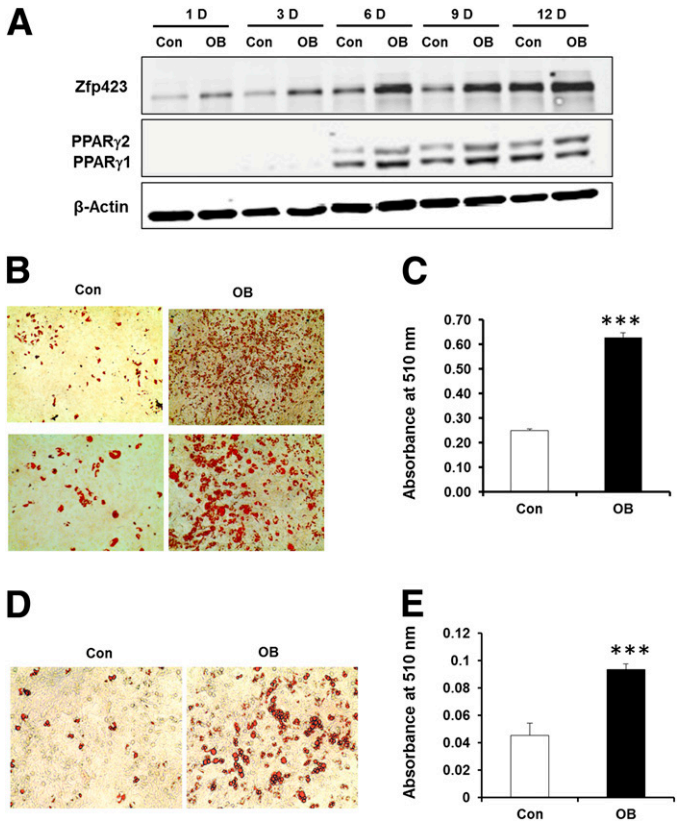

FIG. 2. Adipogenesis of MEFs separated from Con (□) and OB (■) fetal tissue. *A*: Adipogenesis of Con and OB MEFs was induced using standard adipogenic cocktail, and the contents of Zfp423 and PPARγ were analyzed at 0, 3, 6, 9, and 12 days. After 12 days of differentiation, adipocytes derived from Con and OB MEFs were visualized by Oil Red O staining (*top*, ×40 magnification; *bottom*, ×100 magnification) (*B*), and stained Oil Red O dye in MEFs was extracted and measured by spectrometry at 510 nm (*C*). *D* and *E:* MEFs were sorted by Sca-1$^+$/CD45$^-$, adipogenesis of sorted cells was induced for 12 days, and adipocytes were visualized by Oil Red O staining (×100 magnification) (*D*), and stained Oil Red O dye in sorted cells was extracted and measured by spectrometry at 510 nm (*E*). ***P < 0.001. Mean ± SE; n = 5.

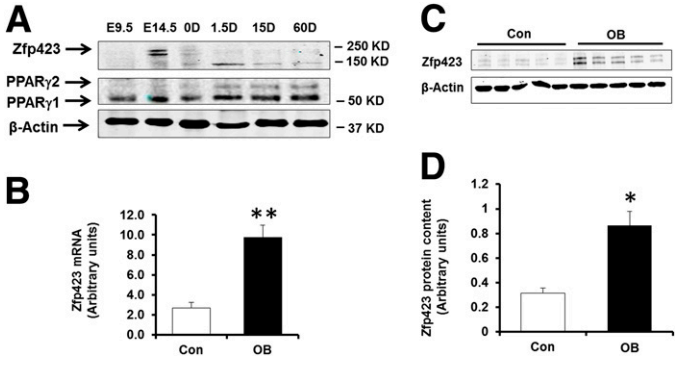

FIG. 1. Zfp423 expression in fetal tissue of Con (□) and OB (■) fetal tissue. *A*: Zfp423 and PPARγ protein contents in fetal and offspring mice (due to the absence of mature adipose tissue in E9.5, E14.5, and 0 day of age [0D] animals, whole fetal tissue was used; for 1.5, 15, and 60 days, adipose tissue was used). *B*: Zfp423 mRNA expression was enhanced in OB mouse. *C* and *D*: OB fetal tissue contained more Zfp423 protein than Con tissue. *P < 0.05; **P < 0.01. Mean ± SE; n = 5.

detected in OB compared with Con sorted progenitor cells (Fig. 2*D* and *E*), consistent with data obtained from MEFs. Of note, the adipogenic capacity of sorted cells was lower than that of MEFs (Fig. 2*B* and *D*), showing that there were additional populations of cells with high adipogenic capacity in fetal tissue. To be inclusive for all cells, for further studies, we used MEFs or fetal tissue, which represents the overall adipogenic commitment in E14.5 fetuses due to MO. This approach fits our objective to explore the impact of MO on Zfp423 expression, associated epigenetic modifications, and the adipogenic commitment during fetal development.

Zfp423 regulates adipogenic differentiation of MEFs. We have demonstrated that MO enhanced Zfp423 expression in OB fetal tissue. The remaining question is whether high Zfp423 expression is critical for enhanced adipogenic differentiation during fetal development. To test this, we prepared MEFs from both Con and OB fetal tissue, which were then transfected with either a vector overexpressing Zfp423 or an shZfp423 plasmid to knockdown Zfp423 mRNA. After 48 h, Zfp423 expression was dramatically increased in Zfp423-transfected cultures, accompanied by

enhanced PPARγ expression. In contrast, knockdown of Zfp423 decreased PPARγ expression compared with MEFs transfected with enhanced green fluorescent protein ($P < 0.05$) (Fig. 3*A*). The same pattern of changes was observed after 6 days (Fig. 3*B*). After 12 days of adipogenic differentiation, many more adipocytes were visually detected in MEFs overexpressing Zfp423 while reduced by Zfp423 knockdown (Fig. 3*C*). Furthermore, comparing Con and OB MEFs, overexpression of Zfp423 was sufficient to enhance adipogenic differentiation of Con MEFs while knockdown of Zfp423 reduced the high adipogenic capacity of OB MEFs (Fig. 3*D*). These data showed that Zfp423 regulates adipogenesis of MSCs and suggest that Zfp423 mediates the effects of MO on the adipogenic differentiation of fetal progenitor cells during development.

DNA methylation of the Zfp423 promoter was lower in OB compared with Con fetal tissue. The next question is why Zfp423 expression was enhanced in OB compared with Con tissue. Through the analysis of ChIP sequencing data, we found that the Zfp423 promoter and its 5′ upstream region had an abundant presence of H3K27me3 and H3K4me3, showing that the Zfp423 promoter is in a bivalent state (Fig. 4*A*). The promoters of genes with bivalent histone modifications may lose active histone modifications and convert to stable DNA methylation when lacking the stimuli to activate gene expression (25). To analyze whether there was a change in DNA methylation, we further analyzed the abundance of CpG sites in the Zfp423 promoter. As expected, exceptionally rich CpG sites were detected in the Zfp423 promoter (Fig. 4*B*). The location of CpG islands overlays with the presence of H3K27me and H3K4me3. To elucidate whether there is a difference in DNA methylation, we compared DNA methylation status using the sodium bisulfite sequencing. Interestingly, DNA methylation was largely absent in CpG sites proximate at the transcription start site (TSS) in both Con and OB tissue, and a higher density of CpG methylation was detected upstream of TSS. Overall, DNA methylation was more abundant in the Zfp423 promoter of the Con compared with the OB tissue (Fig. 4*C*), consistent with the lower Zfp423 expression in Con fetal tissue.

Histone methylation and acetylation in the Zfp423 promoter of Con and OB fetal tissue. PcG protein EZH2 catalyzes inhibitory histone modification, H3K27me3, and further acts as a recruitment platform for DNA methyltransferases (35). To explore mechanisms leading to the reduction of Zfp423 DNA methylation in OB fetal tissue, we analyzed H3K27me3 and H3K4me3 in the Zfp423 promoter. OB decreased H3K27me3 modification in the GC-rich region of the Zfp423 promoter (2.6-fold, $P = 0.01$), showing that PRC2 was likely involved in the epigenetic modifications (Fig. 5*A* and *B*). On the other hand, active H3K4me3 histone marker was significantly higher in the OB fetal tissue (Fig. 5*A*, *C*, and *D*), consistent with reduced Zfp423 methylation and its enhanced expression, as well as reduction of H3K27me3 in the OB tissue (Fig. 4). These data further confirm Zfp423 as a member of genes with bivalent histone modifications, which are known to be critical for early cell commitment and differentiation (24).

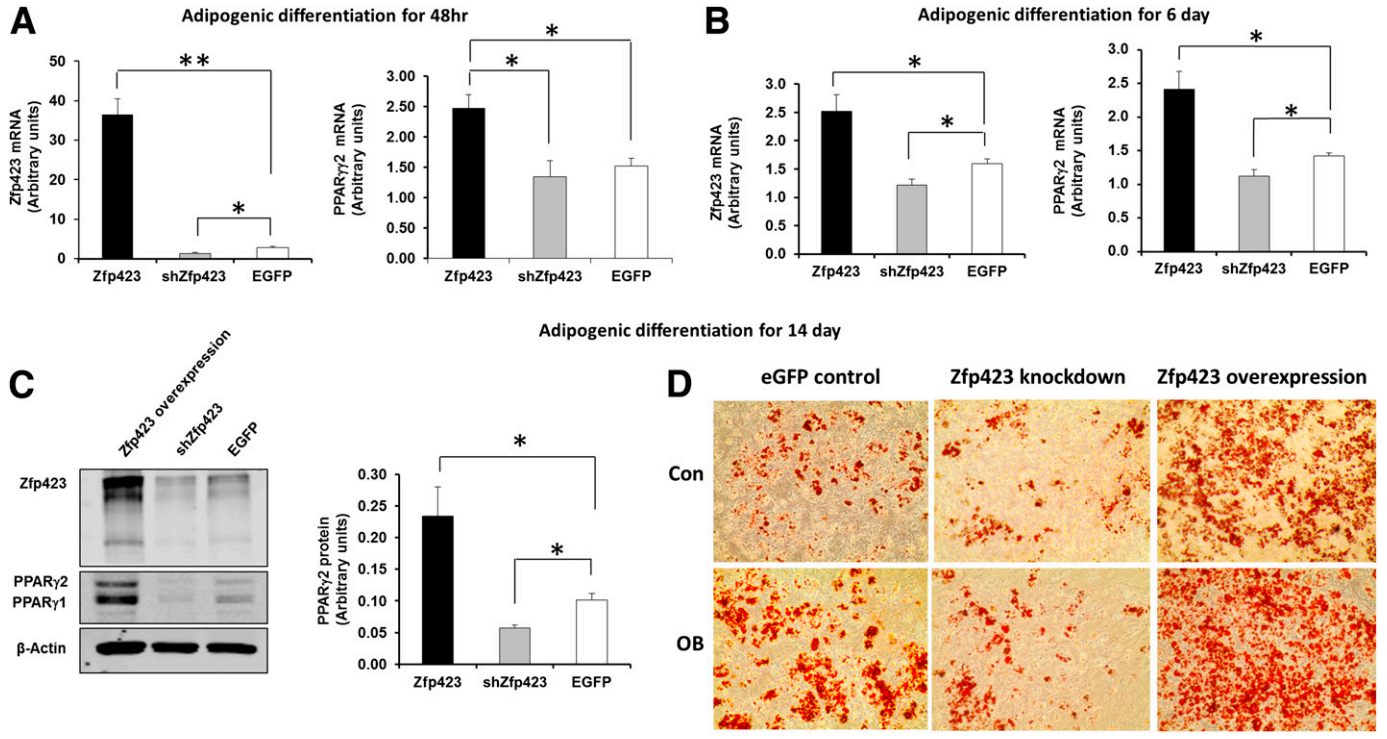

FIG. 3. ZFP423 regulated adipogenic differentiation of MEFs from fetal tissue. MEFs were separated from Con and OB E14.5 fetuses and were transfected with enhanced green fluorescent protein (EGFP) control vector, Zfp423 overexpression vector, or Zfp423 short hairpin RNA vector with target genes driven by the mouse stem cell PCMV virus long terminal repeat (PCMV-LTR), and then adipogenic differentiation was induced. Adipogenic differentiation was induced in MEFs separated from Con E14.5 fetal tissue, and Zfp423 and PPARγ2 expression was analyzed after 48 h (*A*) and 6 days (*B*) and both Zfp423 and PPARγ2 protein contents after 14 days (*C*). *D*: Oil Red O staining of both Con and OB MEFs after 14 days of adipogenic differentiation. Original magnification ×200. *$P < 0.05$; **$P < 0.01$. Mean ± SE; $n = 5$.

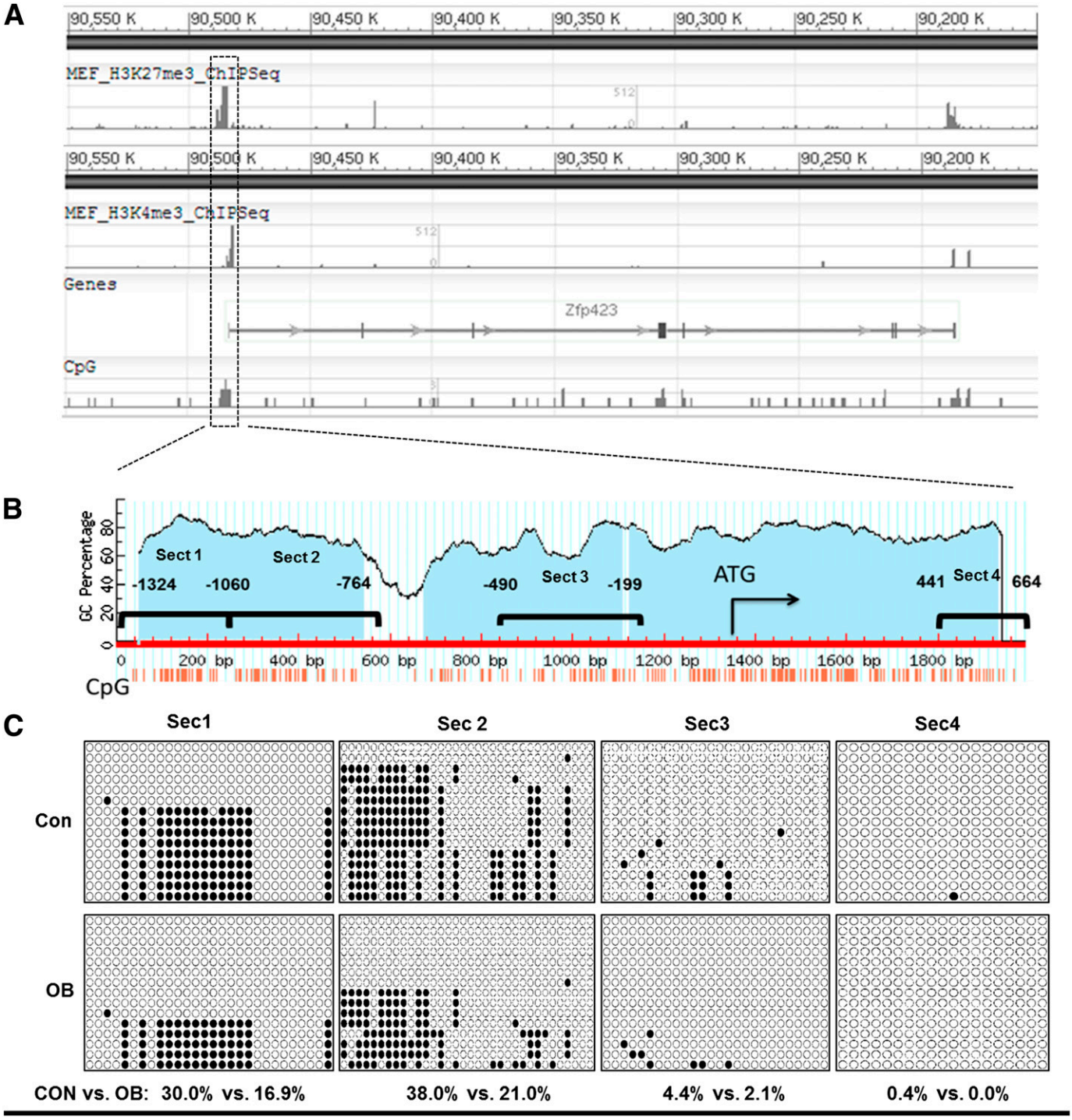

FIG. 4. H3K4me3 and H3K27me3 abundance, CpG sites, and DNA methylation in the Zfp423 promoter of Con (□) and OB (■) fetal tissue. *A*: ChIP-seq data of the Zfp423 promoter region in MEFs. (Bioinformatic analysis was based on genome-wide epigenetic data from the National Center for Biotechnology Information: http://www.ncbi.nlm.nih.gov/epigenomics. Data were accessed by choosing Browse Experiments and choosing Filters, including the following: species, *Mus musculus*; biological source, fibroblasts; and feature type, H3K27me or H3K4me3. Finally, MEF and MEF_ChIPSeq were chosen to view epigenetic modifications on Zfp423.) *B*: The genomic structure and CpG sites of the Zfp423 promoter. Blue regions show CpG islands and short lines represent each CpG dinucleotide, and the regions analyzed by sodium bisulfite sequencing data are shown (45). *C*: Bisulfite genomic sequencing and methylation of the Zfp423 promoter, and percentages of methylated CpG sites (Sec1–Sec4 as shown in *B*; white and black circles indicate unmethylated and methylated CpGs, respectively).

In addition, the binding of Suz12, EZH2, and RNG1B, components of PRC2, was highly enriched in the Zfp423 promoter (Fig. 6*A*). EZH2 catalyzes H3K27me3, and the mRNA expression and protein content of EZH2 were higher in OB compared with Con tissue (Fig. 6*B* and *C*). This was unexpected but consistent with a previous report, where EZH2 expression was shown to be elevated during adipogenic differentiation (36). Despite the increase

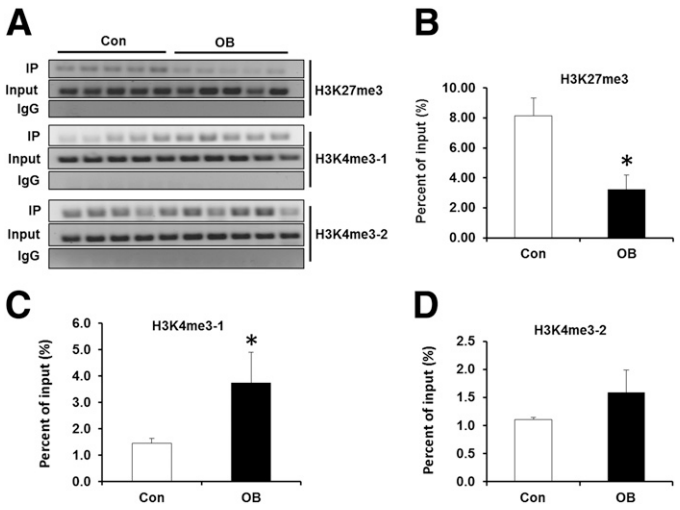

FIG. 5. Histone modifications (H3K27me3 and H3K4me3) in the Zfp423 promoter of Con (□) and OB (■) fetal tissue. Amplicon levels obtained from ChIP–quantitative PCR (ChIP-qPCR) analysis were normalized by that of input genomic DNA content. Normal rabbit IgG was used as the negative control. *A*: Amplicon levels of ChIP-qPCR normalized to the input genomic DNA. *B*: H3K27me3 modification (primers based on −1.3 to −1.5 kb of Zfp423 promoter). *C*: H3K4me3 modification (primers based on −1.3 to −1.5 kb of Zfp423 promoter). *D*: H3K4me3 modification (primers based on −0.6 to −0.75 kb of Zfp423 promoter). *$P < 0.05$. Mean ± SE; $n = 5$.

in overall EZH2 content, MO reduced the binding of EZH2 to the Zfp423 promoter of OB compared with Con fetal tissue, corroborating H3K27me3 and DNA methylation data (Fig. 6*D*).

Active gene expression is associated with enhanced histone acetylations, which were further analyzed (H3K9ac and H3K27ac). There was no difference in H3K27ac, but H3K9ac was higher in the Zfp423 promoter of OB compared with Con tissue (Fig. 7*A* and *B*), accentuating the role of these active epigenetic marks in the heightened Zfp423 expression in OB compared with Con fetal tissue.

Based on these data, we propose that MO reduced the binding of Polycomb group proteins to the Zfp423 promoter, which reduced inhibitory H3K27me3 histone modification and DNA methylation in the promoter, activating Zfp423 expression in fetal progenitor cells to predispose these and their derived cells to adipogenic differentiation (Fig. 7*C*).

DISCUSSION

Obesity is associated with excessive adipose tissue accumulation in three major depots in the body, including visceral, subcutaneous, and intermuscular/intramuscular depots. However, fat accumulation is not evenly distributed to these depots, and the accumulation of fat in the visceral depot is correlated with insulin resistance and the risk for T2D (37,38). In addition, fatty accumulation inside skeletal muscle leads to muscle insulin resistance, which has not been appreciated until recently (39).

Adipose tissue, including both white and brown adipose tissue, is mainly developed during the early developmental stages. Enhancing adipogenic differentiation during fetal development forms more preadipocytes and white adipocytes, which lead to adiposity in specific depots in offspring. In this study, we observed that adipogenic differentiation was enhanced in OB compared with Con fetal tissue, which is consistent with previous studies. MO enhanced adipogenic differentiation in fetal tissue (40,41), and increased intramuscular adipose tissue in MO offspring (42), as well as central adiposity (12,13). Of note, we did not observe an increase in fetal body weight at E14.5, which could be due to the smallness and immaturity of fetuses at this stage. Using the same dietary-induced obesity model, the body weight of neonatal mice of OB was higher than that of Con mice (13), and MO leads long-term obesity in offspring (12,13).

To define the mechanisms leading to the enhanced adipogenic differentiation in OB fetal tissue, we first analyzed whether Zfp423 regulates adipogenic commitment in fetal tissue. To our knowledge, our data, for the first time, suggest that Zfp423 regulates adipogenic commitment and adipogenesis in the developing fetal tissue. The remaining question becomes how MO regulates Zfp423 expression during fetal development. The Zfp423 promoter presents exceptionally rich CpG sites and islands, meeting the characteristics of a "key developmental gene" with high CpG density promoters (24), and previous chromatin immunoprecipitation and parallel sequencing (ChIP-Seq) results showed that during embryonic development, these rich CpG sites recruit PRC2, which catalyzes H3K27me3 in MEFs (43). These data strongly support the notion that MO regulates Zfp423 expression and adipogenesis through altering DNA methylation and other epigenetic modifications. To test this, we designed primers corresponding to the CpG islands overlaying the H3K27me3 peak in the Zfp423 promoter. Indeed, we observed that MO reduced DNA methylation in the Zfp423 promoter. However, DNA methylation in these CpG-rich regions was low and largely unmethylated, especially for regions located on TSS, which was unexpected but in agreement with previous reports that the majority of CpG islands of high CpG genes remain unmethylated or at a low methylation status during differentiation (24), and DNA methylation mainly occurs in the shore area of CpG islands (22). Indeed, we found that the methylation level was much higher in those regions located upstream of TSS. As expected, the DNA methylation was lower in OB compared with Con fetal tissue and negatively associated with the higher expression of Zfp423 in OB fetal tissue.

Stem cells maintain their pluripotency through reversible inhibition of lineage-specific genes while allowing genes needed for self-renewal to express. Conversely, during differentiation, lineage-specific genes are expressed while pluripotency genes are inhibited (25). PRCs are mainly responsible for reversible inhibition of genes. There are two well-characterized PRCs, PRC1 and PRC2. PRC2 tends to bind promoters with rich GC sites, which attracts PRC1 binding (22,25). Because the Zfp423 promoter has exceptionally rich GC sites, PRC2 is positioned as a key mediator of Zfp423 expression and adipogenic commitment, which induces H3K27me3 (21). De novo DNA methylation serves to convert plastic gene inhibition by PRCs to permanent silencing (25). Our data show that the H3K27me3 and EZH2 levels in the Zfp423 promoter were lower in OB compared with Con fetal tissue, consistent with the lower DNA methylation and the high expression of Zfp423. However, it is surprising that total EZH2 expression in OB was higher than in Con tissue; nevertheless, this result is consistent with a previous report (36). These data suggest that the specific binding of EZH2 to the Zfp423 promoter, not the EZH2 content, is critical for the

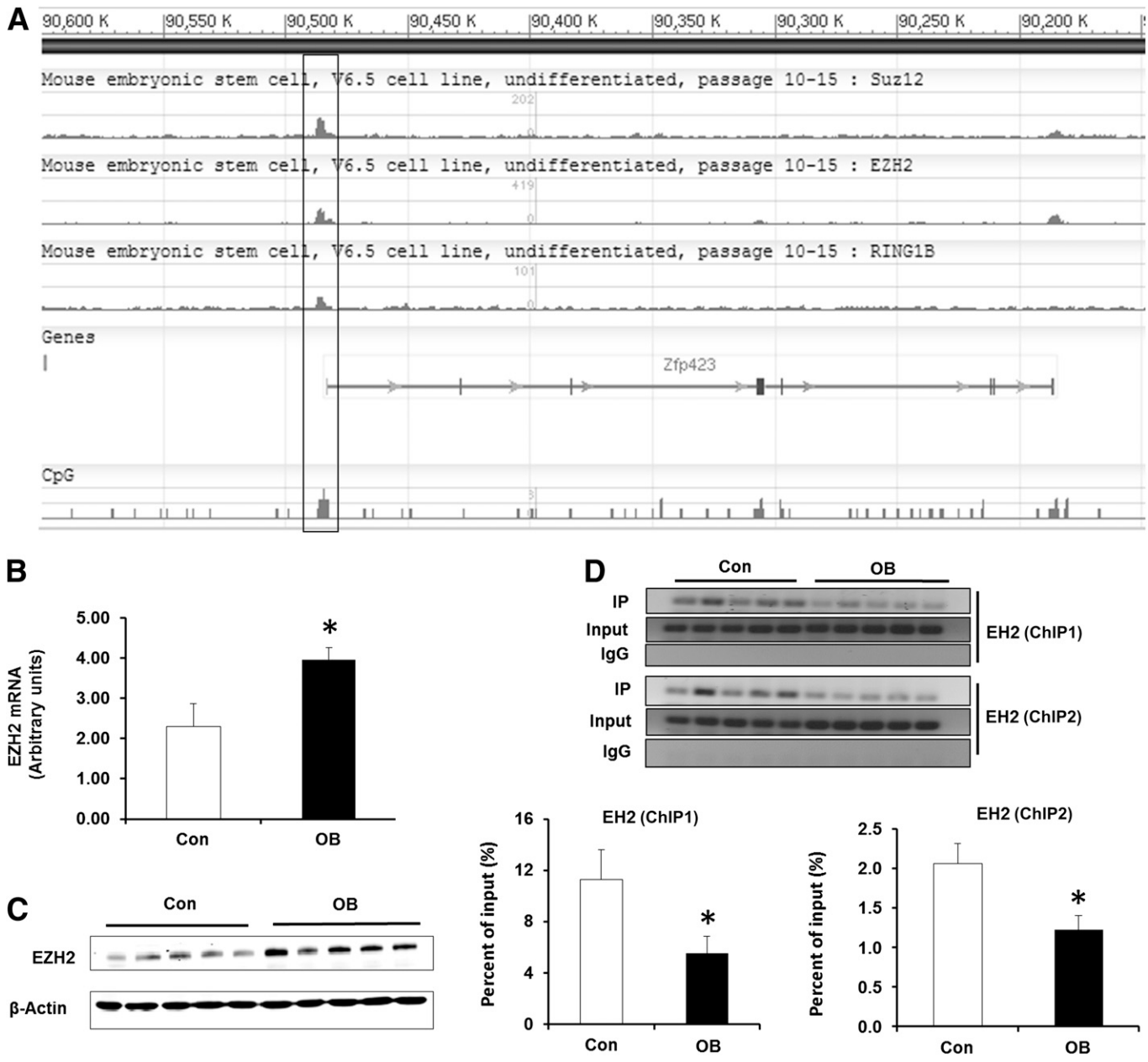

FIG. 6. Abundance of EZH2 and other Polycomb group proteins in the Zfp423 promoter of Con (□) and OB (■) fetal tissue. *A*: Enrichment of Polycomb group proteins, EZH2, Suz12, and RING1B in the Zfp423 promoter. (Bioinformatic analysis is based on the genome-wide epigenetic data from the National Center for Biotechnology Information, as described in the Fig. 4 legend.) *B* and *C*: EZH2 mRNA expression and protein content were higher in OB samples. *D*: Less abundance of EZH2 in the Zfp423 promoter of OB samples. Two ChIP-Seq assays were conducted using primers based on −0.6 to −0.75 and −1.3 to −1.5 kb of the Zfp423 promoter. *$P < 0.05$. Mean ± SE; $n = 5$. IP, immunoprecipitation.

epigenetic modifications in the Zfp423 promoter, which warrants further studies.

TrxG catalyzes H3K4 trimethylation (H3K4me3), which activates gene transcription. It appears that H3K4me3 is transient, and only induced when gene expression is needed to counter the inhibitory effect of the Polycomb group (23,44). The level of H3K4me3 in the Zfp423 promoter was slightly higher in OB fetal tissue, which indicates that trxG was also involved in the control of Zfp423 expression due to MO but appeared minor compared with PRC2.

In summary, for the first time, we observed that MO reduced DNA methylation in the Zfp423 promoter, which was correlated with higher Zfp423 expression and enhanced adipogenesis of progenitor cells. We further show that histone modification, H3K27me3, a reaction catalyzed by PRC2, was lower in OB fetal tissue, which provides a mechanism for the reduced DNA methylation in the Zfp423 promoter, and enhanced Zfp423 expression and adipogenesis in OB fetal tissue. Because DNA methylation is stable, the reduced DNA methylation in the Zfp423 promoter and enhanced Zfp423 expression in fetal progenitor cells likely enhance the adipogenic capacity of their derived cells in offspring adipose tissue, predisposing offspring to adiposity and the accompanied metabolic dysfunction, which might partially explain the increasing rates of obesity and even T2D in teenagers and even children.

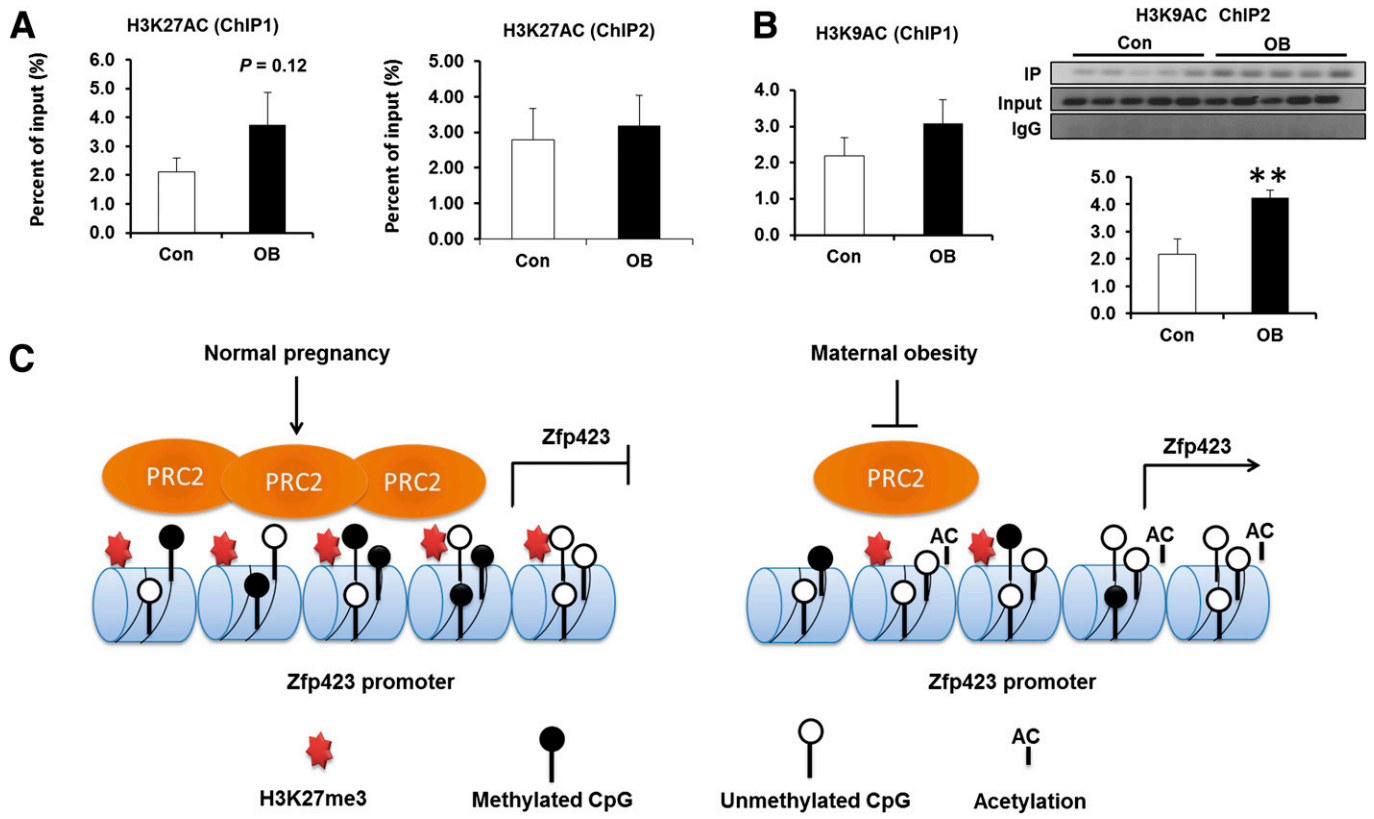

FIG. 7. Histone acetylation and the proposed model for epigenetic modifications in the Zfp423 promoter of Con (□) and OB (■) fetal tissue. *A*: H3K27 acetylation (H3K27AC) tended to be higher in OB samples, demonstrated by two ChIP assays with primers based on −0.6 to −0.75 and −1.3 to −1.5 kb of the Zfp423 promoter. *B*: H3K9 acetylation (H3K9AC) was higher in OB samples, demonstrated by two ChIP assays with primers based on −0.6 to −0.75 and −1.3 to −1.5 kb of the Zfp423 promoter. *C*: Proposed model for the effects of MO on epigenetic modifications in the Zfp423 promoter, which enhances Zfp423 expression and adipogenic differentiation of progenitor cells. **$P < 0.01$. Mean ± SE; $n = 5$.

ACKNOWLEDGMENTS

This work was funded by National Institutes of Health grant R01-HD-067449.

No potential conflicts of interest relevant to this article were reported.

Q.-Y.Y. researched data and wrote the manuscript. J.-F.L. researched data. C.J.R. and J.-X.Z. contributed to discussion. M.-J.Z. contributed to discussion and reviewed and edited the manuscript. M.D. wrote the manuscript and designed the experiments. M.D. is the guarantor of this work and, as such, had full access to all the data in the study and takes responsibility for the integrity of the data and the accuracy of the data analysis.

REFERENCES

1. Flegal KM, Carroll MD, Kit BK, Ogden CL. Prevalence of obesity and trends in the distribution of body mass index among US adults, 1999-2010. JAMA 2012;307:491–497
2. Fowden AL, Ward JW, Wooding FP, Forhead AJ, Constancia M. Programming placental nutrient transport capacity. J Physiol 2006;572:5–15
3. Barker DJ. Fetal programming of coronary heart disease. Trends Endocrinol Metab 2002;13:364–368
4. Desai M, Beall M, Ross MG. Developmental origins of obesity: programmed adipogenesis. Curr Diab Rep 2013;13:27–33
5. Bayol SA, Simbi BH, Bertrand JA, Stickland NC. Offspring from mothers fed a 'junk food' diet in pregnancy and lactation exhibit exacerbated adiposity that is more pronounced in females. J Physiol 2008;586:3219–3230
6. Petersen KF, Dufour S, Shulman GI. Decreased insulin-stimulated ATP synthesis and phosphate transport in muscle of insulin-resistant offspring of type 2 diabetic parents. PLoS Med 2005;2:e233
7. Ross R, Berentzen T, Bradshaw AJ, et al. Does the relationship between waist circumference, morbidity and mortality depend on measurement protocol for waist circumference? Obes Rev 2008;9:312–325
8. Greenwood MR, Hirsch J. Postnatal development of adipocyte cellularity in the normal rat. J Lipid Res 1974;15:474–483
9. Johnson PR, Hirsch J. Cellularity of adipose depots in six strains of genetically obese mice. J Lipid Res 1972;13:2–11
10. Hoffstedt J, Arner E, Wahrenberg H, et al. Regional impact of adipose tissue morphology on the metabolic profile in morbid obesity. Diabetologia 2010;53:2496–2503
11. Modi N, Murgasova D, Ruager-Martin R, et al. The influence of maternal body mass index on infant adiposity and hepatic lipid content. Pediatr Res 2011;70:287–291
12. Samuelsson AM, Matthews PA, Argenton M, et al. Diet-induced obesity in female mice leads to offspring hyperphagia, adiposity, hypertension, and insulin resistance: a novel murine model of developmental programming. Hypertension 2008;51:383–392
13. Tong JF, Yan X, Zhao JX, Zhu MJ, Nathanielsz PW, Du M. Metformin mitigates the impaired development of skeletal muscle in the offspring of obese mice. Nutr Diabetes 2011;1:e7
14. Lowell BB, Shulman GI. Mitochondrial dysfunction and type 2 diabetes. Science 2005;307:384–387
15. Miljkovic I, Kuipers AL, Kammerer CM, et al. Markers of inflammation are heritable and associated with subcutaneous and ectopic skeletal muscle adiposity in African ancestry families. Metab Syndr Relat Disord 2011;9:319–326
16. Miljkovic I, Cauley JA, Petit MA, et al.; Osteoporotic Fractures in Men Research Group; Tobago Health Studies Research Group. Greater adipose tissue infiltration in skeletal muscle among older men of African ancestry. J Clin Endocrinol Metab 2009;94:2735–2742
17. Hosoyama T, Ishiguro N, Yamanouchi K, Nishihara M. Degenerative muscle fiber accelerates adipogenesis of intramuscular cells via RhoA signaling pathway. Differentiation 2009;77:350–359
18. Du M, Yan X, Tong JF, Zhao J, Zhu MJ. Maternal obesity, inflammation, and fetal skeletal muscle development. Biol Reprod 2010;82:4–12

19. Rosen ED, Sarraf P, Troy AE, et al. PPAR gamma is required for the differentiation of adipose tissue in vivo and in vitro. Mol Cell 1999;4:611–617
20. Gupta RK, Arany Z, Seale P, et al. Transcriptional control of preadipocyte determination by Zfp423. Nature 2010;464:619–623
21. Bernstein BE, Mikkelsen TS, Xie X, et al. A bivalent chromatin structure marks key developmental genes in embryonic stem cells. Cell 2006;125:315–326
22. Mendenhall EM, Koche RP, Truong T, et al. GC-rich sequence elements recruit PRC2 in mammalian ES cells. PLoS Genet 2010;6:e1001244
23. Schuettengruber B, Martinez AM, Iovino N, Cavalli G. Trithorax group proteins: switching genes on and keeping them active. Nat Rev Mol Cell Biol 2011;12:799–814
24. Meissner A, Mikkelsen TS, Gu H, et al. Genome-scale DNA methylation maps of pluripotent and differentiated cells. Nature 2008;454:766–770
25. Mohn F, Weber M, Rebhan M, et al. Lineage-specific polycomb targets and de novo DNA methylation define restriction and potential of neuronal progenitors. Mol Cell 2008;30:755–766
26. Zhao J, Yue W, Zhu MJ, Sreejayan N, Du M. AMP-activated protein kinase (AMPK) cross-talks with canonical Wnt signaling via phosphorylation of β-catenin at Ser 552. Biochemic Biophys Res Commun 2010;395:146–151
27. Li LC, Dahiya R. MethPrimer: designing primers for methylation PCRs. Bioinformatics 2002;18:1427–1431
28. Kumaki Y, Oda M, Okano M. QUMA: quantification tool for methylation analysis. Nucleic Acids Res 2008;36:W170–W175
29. Uchida T, Furumai K, Fukuda T, et al. Prolyl isomerase Pin1 regulates mouse embryonic fibroblast differentiation into adipose cells. PLoS ONE 2012;7:e31823
30. Saeed H, Taipaleenmäki H, Aldahmash AM, Abdallah BM, Kassem M. Mouse embryonic fibroblasts (MEF) exhibit a similar but not identical phenotype to bone marrow stromal stem cells (BMSC). Stem Cell Rev 2012;8:318–328
31. Miyoshi H, Souza SC, Zhang HH, et al. Perilipin promotes hormone-sensitive lipase-mediated adipocyte lipolysis via phosphorylation-dependent and -independent mechanisms. J Biol Chem 2006;281:15837–15844
32. Okazaki H, Osuga J, Tamura Y, et al. Lipolysis in the absence of hormone-sensitive lipase: evidence for a common mechanism regulating distinct lipases. Diabetes 2002;51:3368–3375
33. Dupas T, Rouaud T, Rouger K, et al. Fetal muscle contains different CD34+ cell subsets that distinctly differentiate into adipogenic, angiogenic and myogenic lineages. Stem Cell Res (Amst) 2011;7:230–243
34. Montarras D, Morgan J, Collins C, et al. Direct isolation of satellite cells for skeletal muscle regeneration. Science 2005;309:2064–2067
35. Viré E, Brenner C, Deplus R, et al. The Polycomb group protein EZH2 directly controls DNA methylation. Nature 2006;439:871–874
36. Wang L, Jin Q, Lee JE, Su IH, Ge K. Histone H3K27 methyltransferase Ezh2 represses Wnt genes to facilitate adipogenesis. Proc Natl Acad Sci USA 2010;107:7317–7322
37. Einstein FH, Fishman S, Muzumdar RH, Yang XM, Atzmon G, Barzilai N. Accretion of visceral fat and hepatic insulin resistance in pregnant rats. Am J Physiol Endocrinol Metab 2008;294:E451–E455
38. Klein S. Is visceral fat responsible for the metabolic abnormalities associated with obesity?: implications of omentectomy. Diabetes Care 2010;33:1693–1694
39. Aguiari P, Leo S, Zavan B, et al. High glucose induces adipogenic differentiation of muscle-derived stem cells. Proc Natl Acad Sci USA 2008;105:1226–1231
40. Zhu MJ, Han B, Tong J, et al. AMP-activated protein kinase signalling pathways are down regulated and skeletal muscle development impaired in fetuses of obese, over-nourished sheep. J Physiol 2008;586:2651–2664
41. Yan X, Zhu MJ, Xu W, et al. Up-regulation of Toll-like receptor 4/nuclear factor-kappaB signaling is associated with enhanced adipogenesis and insulin resistance in fetal skeletal muscle of obese sheep at late gestation. Endocrinology 2010;151:380–387
42. Yan X, Huang Y, Zhao JX, et al. Maternal obesity-impaired insulin signaling in sheep and induced lipid accumulation and fibrosis in skeletal muscle of offspring. Biol Reprod 2011;85:172–178
43. Goren A, Ozsolak F, Shoresh N, et al. Chromatin profiling by directly sequencing small quantities of immunoprecipitated DNA. Nat Methods 2010;7:47–49
44. Eissenberg JC, Shilatifard A. Histone H3 lysine 4 (H3K4) methylation in development and differentiation. Dev Biol 2010;339:240–249
45. Ku M, Koche RP, Rheinbay E, et al. Genomewide analysis of PRC1 and PRC2 occupancy identifies two classes of bivalent domains. PLoS Genet 2008;4:e1000242